

Microindentation technique as a tool for investigating the development of order in PET under uniaxial stress

Ahmed I. Abou-Kandil · A. Flores · F. J. Balta Calleja ·
A. H. Windle

Received: 21 September 2007 / Accepted: 11 February 2008 / Published online: 28 February 2008
© Springer Science + Business Media B.V. 2008

Abstract The development of microhardness during annealing was used as a tool to follow the development of the liquid crystalline transient mesophase during the crystallization of uniaxially oriented polyethylene terephthalate (PET). 2D X-ray diffraction was used to characterize the different stages of the crystallization process. We were able to separate those stages by quenching into air. Microindentation hardness experiments were done in real time where samples were heated with their ends fixed on a specially developed stage and microhardness was measured simultaneously. The oriented samples examined exhibit a clear difference in behavior from isotropic samples that mainly lack the existence of such an ordered mesophase. The mesophase clearly has a reinforcement effect on the whole polymer matrix that leads to an increase in hardness value with annealing of the oriented PET films. Microindentation hardness is shown to be a versatile tool to detect the existence of the liquid crystalline transient mesophase. It is also efficient in

comparing and explaining results obtained by wide angle X-ray scattering.

Keywords Microhardness · PET · Crystallization · Mesophase · Order · Uniaxial stress

Introduction

The current understanding of polymer crystallisation is moving towards a picture in which ordering takes place in stages involving one or more intermediate stages, broadly termed as *mesophases*. Although the concept is quite old, having been recognised already by Ostwald in his rule of stages in the late 19th Century, it has only gathered recognition in polymer crystallisation field in recent years.

Early models of the staged ordering in polyethylene terephthalate (PET) described by Bonart [1] remained largely unnoticed until recently. In 1995 Imai et al. [2] suggested an initial ordering of unoriented samples of PET into *nematic* like regions in a *spinodal* decomposition process followed by crystallisation.

Auriemma et al. [3] and Nicholson et al. [4], attempted to model the structure of the PET mesophase. They suggested the existence of two stable structures for PET. In one structure the PET chains are fully extended, corresponding to the usual triclinic form and an alternative conformation, where the dihedrals between the CO–O–C are rotated by about 80°.

Studies published by Welsh et al. [5, 6], indicated the ability of presence of the mesophase in the 50/50 PET/polyethylene naphthalate (PEN) copolymer fibres drawn at 100 °C to draw ratios (DR) of 6 and 10. Also recent studies by Mahendrasigam et al. [7] and Blundell et al. [8] conducted on PET, PEN and 50% PET/PEN random

A. I. Abou-Kandil · A. H. Windle
Department Of Materials Science and Metallurgy,
University of Cambridge,
Pembroke Street,
Cambridge CB2 3QZ, UK

A. Flores · F. J. Balta Calleja
Instituto de Estructura de la Materia, CSIC,
Serrano, 119,
28006 Madrid, Spain

Present address:

A. I. Abou-Kandil (✉)
Max-Planck Institute for Polymer Research,
Ackermannweg 10,
Mainz 55128, Germany
e-mail: aia_23@yahoo.co.uk

copolymer have also confirmed the existence of such a mesophase.

Abou-Kandil et al. [9] studied in detail the development of microstructure during the annealing of oriented PET films using X-ray scattering techniques. These results concluded that there is a uniform global change taking place over the entire sample during the transition between oriented amorphous and oriented crystalline states. The Wide Angle X-ray Scattering (WAXS) results discussed indicated the presence of an intermediate liquid crystalline phase prior to crystallization. The mesophase was classified as having a smectic-A type order. On the other hand the small Angle X-ray Scattering (SAXS) results from the mesophase suggested the presence of fibrillar arrangement of the polymer chains in the direction of the draw. This was represented by the initial fibre streaking, but it gave no evidence of density variation which would indicate the presence of significant microstructure. However, once crystallization started on annealing above the glass transition temperature, the SAXS showed very clear evidence of microstructure which then developed. We also studied the morphology using scanning electron microscope [10] and used molecular modelling to validate the structure of the mesophase and compare the resulting diffraction patterns it to the experimental data [11].

Asano et al. [12] have used hardness measurements to distinguish between the different phases occurring during the crystallization of oriented PET. In their experiments all measurements have been done at room temperature and it showed that the hardness of PET increased by increasing the annealing temperature and that the indentation anisotropy decreases when PET samples are annealed at temperatures above glass transition (T_g). The aim of our present paper is to examine the microhardness behaviour of the oriented glassy PET, in real time, as a function of temperature. We intend to contribute to the understanding of the role of the transient mesophase in the crystallization process.

Microhardness of oriented polymers

Microindentation using a point indenter involving a deformation on a very small scale is one of the simplest methods for determining the microhardness, H , of a material. The method uses a diamond pyramid indenter that penetrates the surface of the specimen upon application of a given load at a constant rate. A convenient measure of H may be obtained by dividing the peak contact load, P , by the projected area of deformation, A , $H = P/A$. Detailed description of the measurement will be explained in “Experimental” below.

Uniaxial mechanical deformation provokes drastic changes in the indentation pattern of drawn polymers. The

newly created fibre structure consists of highly aligned microfibrils within the microfibrillar stacks of crystal blocks perpendicularly oriented to the draw direction. The aligned microfibrils act as cross-links for the molecules, bridging adjacent crystalline layers.

Two well-defined hardness values can be defined due to orientation [12, 13]. One value, maximum ($H_{//}$), derived from the indentation diagonal parallel to the fibre axis ($d_{//}$), the second one, minimum (H_{\perp}), is deduced from the diagonal perpendicular to it (d_{\perp}). The former value is in fact not a physical measure of hardness, but corresponds to an instant elastic recovery of the fibrous network in the draw direction. The latter value defines the plastic component of the oriented material. From the morphology of the fibrous structure of the deformed polymer one concludes that the dominant deformation modes of the drawn polymer under the stress field of the indenter involve:

1. Sliding motion of fibrils and microfibrils, which are sheared and displaced normal to the fibre axis under compressive load.
2. Buckling of fibrils parallel to the fibre axis. Since the shape of the indentation must conform with that of the diamond indenter while the load is applied, the anisotropy observed must arise instantly upon load removal because of greater elastic recovery of the fibrillar network with strained molecules along the fibre axis where the stress is largest.

Indentation anisotropy, ΔH , is defined as:

$$\Delta H = 1 - \frac{H_{\perp}}{H_{//}} \quad (1)$$

Experimental

Microhardness measurements

PET samples having three different molecular weights are used in the microindentation experiments. The intrinsic viscosity of PET used is 0.9, 0.65 and 0.45 as given by the supplier, ICI. The molecular weight of the polymer was found to be about 82,000, 50,000 and 28,000 g/mol respectively. The molecular weight was calculated using Kuhn-Mark-Houwink equation [14]:

$$[\eta] = \kappa M_v^{\alpha} \quad (2)$$

The constants for PET are $\alpha=0.695$ and $\kappa = 5.2 \times 10^{-4}$ ml/g [15].

Different oriented amorphous polymer samples were mounted on a hot stage (Mettler FP52) under a microindenter with a square diamond tester. The samples were fixed on an aluminium stage on top of the heating stage by

means of a double-sided temperature resistant adhesive tape to ensure the surface of the sample remains flat during the experiment. The ends of the samples were also fixed with double screws at the edge of the aluminium stage to prevent the oriented sample from shrinkage.

Microindentation experiments were carried out using a Vickers square based diamond pyramid approximately 200 μm in height. The included angles between opposite faces, 2α , equals 136° . A typical load of 0.05 N using this indenter would produce a penetration depth, h_p , of about 3–4 μm in PET samples. Vickers hardness is calculated according to the expression:

$$H = k \frac{P}{d^2} \quad (3)$$

Where P is the load applied, d is the measured diagonal of the residual impression and k is a geometric constant. A value of $k=1.854$ is used when P is in Newton and d is in millimeter to give H in molar pascal.

A loading cycle of 0.1 min is used to minimise creep [16]. The sample thickness was always seven to ten times greater than the measured diagonal values in order to make sure that the measurements taken are the real hardness of the samples without interference of the surface on which the samples were fixed [17]. At least three different loads for each sample were used that verifies the above condition, ranging from 0.147° N to 2.942° N. This was necessary during the microindentation measurement to make sure the value of $\frac{P}{d^2}$ was maintained constant and to correct for the instantaneous elastic recovery of the polymer at high temperatures if necessary [18].

The temperature at the surface of the sample was calibrated against several standards. Sputtering of the sample surface using gold was performed to improve optical contrast during the indentation.

X-ray diffraction

Five different samples have been prepared from 500 μm thick PET films. Each sample was chosen to represent a specific stage observed in the WAXS analysis described in references [9–11]. These stages are: amorphous, oriented amorphous, mesophase, oriented crystalline and oriented crystalline annealed.

In order to prepare each microstructural stage, each sample was drawn to a specific draw ratio at a given temperature and then quickly quenched to air or annealed with the ends fixed at a given temperature. Figure 1 illustrates how each sample was prepared and shows a diffraction 2D diffraction pattern for each sample after preparation.

The X-ray measurements were done on a Philips PW 1729 X-ray generator using a graphite filtered copper K_α X-ray tube producing radiation with a wavelength of 1.54 \AA .

The measurements were made in transmission mode, using a CCD camera as a detector. The sample-to-film distance was calibrated using silicon powder that gives a sharp (100) ring at a 2θ value of 28.442° (d -value of 3.135 \AA).

Results and discussion

Microindentation hardness has been shown to be a valuable tool capable of distinguishing between the amorphous, smectic and crystalline structure of annealed cold drawn PET films after cooling the sample at room temperature [12] as well as unoriented PET and PEN samples [19, 20]. What we are interested in now is to perform the experiments in real time as a function of temperature and time so that we understand the effect of the intermediate liquid crystalline mesophase on the crystallization process. The results to be obtained here are to be interpreted in accordance with the X-ray scattering results obtained [9].

Figure 1 shows the key stages occurring on uniaxially drawing PET at either 40°C or room temperature to a draw ratio of 3.5 and subsequently annealing the sample with its ends fixed. It is clear from the figure that the starting sample is amorphous. This is indicated by the obvious diffuse amorphous halo indicating the absence of crystallinity in the sample, as shown in the 2D WAXS patterns in Fig. 1a. Drawing leads to the orientation of the polymer in the direction of the draw, and the amorphous halo is concentrated on the equator as shown in Fig. 1b.

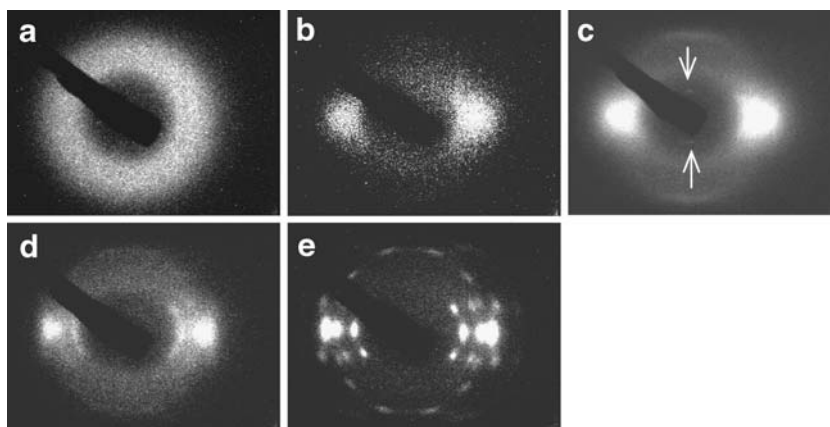
Subsequent annealing leads to the formation of the smectic mesophase, Fig. 1c. The mesophase acts as a precursor to triclinic crystals [5, 6, 9–11]. The key aspects of Fig. 1c are the high degree of orientation and the almost complete absence of crystallisation. The presence of a sharp meridional peak at a position equivalent to 10.42 \AA and the absence of the crystalline order in the interchain packing means that the sample has order which could well be classified as *smectic A*. A more detailed explanation of the development of structure using X-ray diffraction can be found in references [9–11].

Figure 1d represents the oriented crystalline sample drawn to a draw ratio of 3 where it is obvious that there is a hint of splitting starting to take place in the equatorial reflections indicating the existence of horizontal register between the chains and low, two-dimensional, crystallinity.

Figure 1e on the other hand obtained by annealing the oriented crystalline sample at 190°C for 24 h shows distinct splitting of the equatorial reflection into three distinct reflections indicating lateral packing of the chains. The clear first layer lines indicate the development of three-dimensional crystalline structure.

It is of extreme importance also to compare those results with the ones obtained for isotropic polymer samples [18, 21].

Fig. 1 Wide angle X-ray scattering patterns showing the key staged of development of microstructure during drawing of amorphous PET at 40 °C to a draw ratio of 3.5 and then subsequent annealing of the sample with its ends fixed to prevent shrinkage. **a** Amorphous, **b** Oriented Amorphous, **c** Mesophase, **d** Oriented Crystalline, **e** Oriented Annealed



Development of microhardness with temperature

Oriented amorphous samples were clamped on the Aluminium heating stage as explained above; the temperature was raised at 2 °C min⁻¹ and left to equilibrate every 5 °C for 3 min, afterwards the measurements of both $d_{//}$ and d_{\perp} were made.

Development of microhardness in oriented PET

Measuring the microindentation hardness for oriented amorphous PET samples drawn at 40 °C during annealing revealed the behaviour shown in Fig. 2. It is clear that $H_{//}$ values are greater than those of H_{\perp} . This is the consequence of the instant elastic recovery of the fibrils after removal of the indenter, and therefore contributes to the smaller indentation diagonal in the direction perpendicular to the fibre axis. The microhardness values in this case appear to be unchanged until 65 °C, then they start to increase abruptly until the temperature reaches 100 °C, afterwards the increase is less steep and appears to level off. The behaviour is the same for both $H_{//}$ and H_{\perp} . As expected, the microhardness values increase by increasing the molecular weight of the PET samples, which was also observed in an earlier study [14].

Similar behaviour is observed for samples that were drawn at room temperature, shown in Fig. 3. The only difference is that microhardness values in this case do not level off at around 120 °C as observed for samples drawn at 40 °C. This might be because drawing the samples at lower temperature decreases the ability of the polymer chains to align in the direction of the draw. Consequently, they need longer times and higher temperatures to reach an equilibrium state.

Figure 4 illustrates the variation of indentation anisotropy as a function of temperature for the series of PET

samples; anisotropy is a measure of the elastic recovery of the material as discussed above. The first finding in Fig. 4 is the unusually high ΔH values for the samples investigated compared to those reported for PET in earlier studies [12]. However, in those experiments all the measurements were made at room temperature after annealing the samples at certain temperatures. As an average behaviour for all three PET samples under consideration, the values of ΔH start at about 0.4 and then increase gradually with temperature until they reach values as high as 0.6 at 80 °C ($\approx T_g$ of PET) before starting to drop to values comparable to the initial ones.

Influence of temperature on microhardness

From Figs. 3 and 4 four regions of $H_{//}$ and H_{\perp} values can be observed which correlate to various structures as the temperature is increased:

1. $Temperatures \leq 65$ °C: from the WAXS results presented in an earlier study [9] it is clear that the smectic mesophase is present at these temperatures after orientation of the sample. The values of both $H_{//}$ and H_{\perp} appear to be unaffected by the structural changes occurring at these temperatures leading to the approximate levelling of the microhardness values. This behaviour is comparable with that observed for isotropic PET below T_g , where the hardness values remain approximately unchanged with increasing temperature [19, 21].
2. 65 °C < $Temperature \leq 80$ °C: the hardness values increase steadily. Within this temperature range the amount of mesophase present is sufficient to produce an appreciable increase in hardness by reinforcing the structure.
3. 80 °C < $Temperature \leq 100$ °C: the hardness values increase steeply and this is associated with the

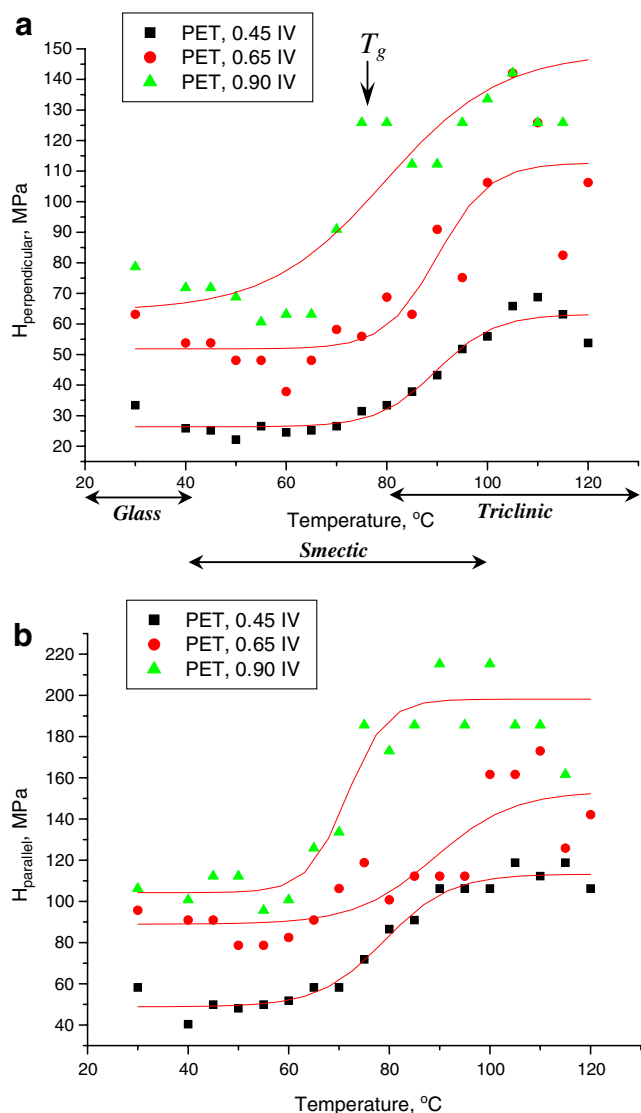


Fig. 2 The development of (a) and H_{\perp} (b) as a function of temperature for different PET samples drawn at 40 °C to a draw ratio of 3.5. [The red curves serve as a guide for the eye]

formation of the triclinic crystals and the start of the disappearance of the smectic domains.

4. $Temperature \geq 100 \text{ }^{\circ}\text{C}$: the smectic phase completely disappears and a three dimensional crystalline order develops as discussed in a previous publication [9]. This is associated with the approximate levelling of hardness values for samples drawn at 40 °C or continuing to increase in high molecular weight PET drawn at room temperature. These results are in contrast to those reported for isotropic PET [19, 21], where the hardness values drop abruptly after T_g due to the softening of the material.

From the above results it can be clearly seen that at low temperatures ($\leq T_g$) the increase in hardness could be

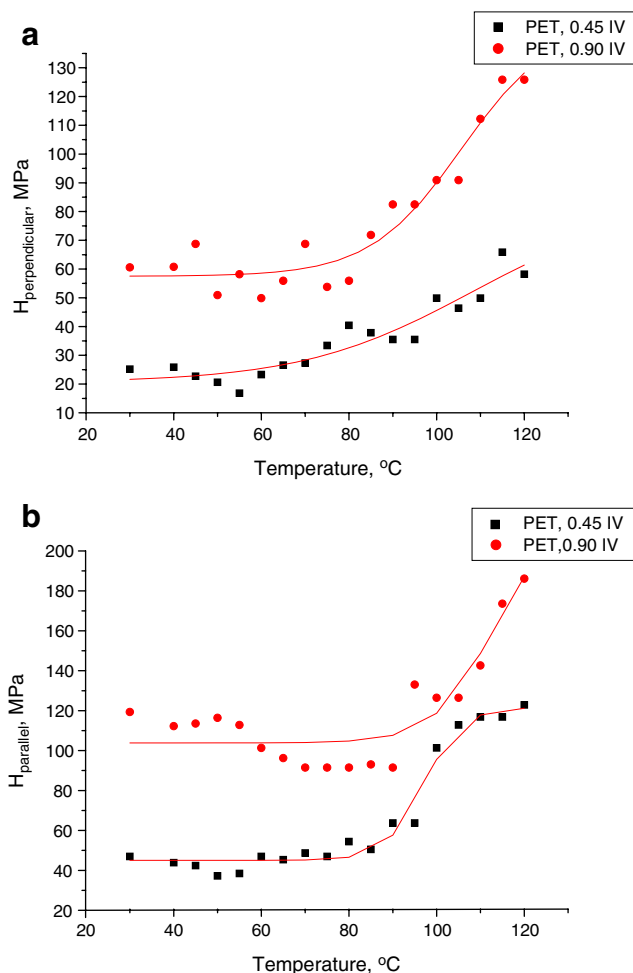


Fig. 3 The development of (a) and H_{\perp} (b) as a function of temperature for different PET samples drawn at room temperature to a draw ratio of 3.5. [The red curves serve as a guide for the eye]

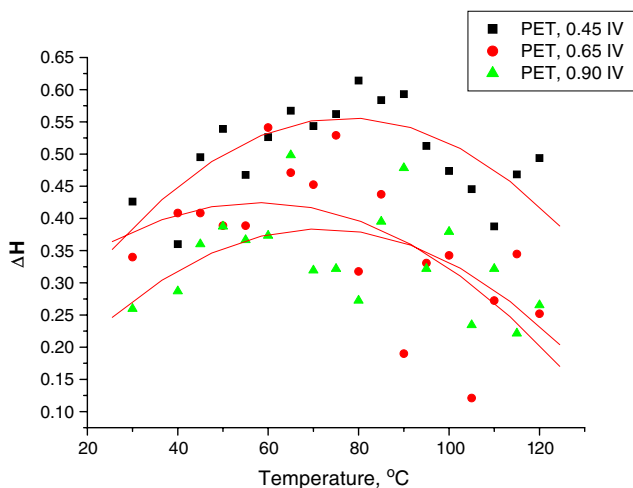


Fig. 4 The development of ΔH as a function of temperature for different PET samples drawn at 40 °C to a draw ratio of 3.5. [The red curves serve as a guide for the eye]

associated with the increase in the smectic order and the possible densification of the smectic domains. On the other hand, at temperatures above T_g the increase in hardness appears to be associated with the increase in crystallinity, and it levels off with the levelling of the crystallinity value.

Influence of temperature on indentation anisotropy

The results shown in Fig. 4 show that in all three PET samples the indentation anisotropy passes through a maximum at about T_g of PET i.e. at around the temperature where the amount of mesophase present in the sample is a maximum.

The initial increase in the value of ΔH with temperature might be due to the increase in the value of H_{\perp} , due to the increase in the mesophase content, it reaches a maximum when the amount of mesophase is maximum and then starts to decline again due to the decrease in the elastic recovery of the material in the chain direction i.e. the decrease of the value of $H_{//}$. Similar behaviour was observed above T_g for PET in an earlier study [12].

Kinetics of mesophase and crystallisation development

The polymer samples were held at constant temperature with their ends fixed to prevent sample shrinkage at high temperature. The sample temperature was raised at $2\text{ }^{\circ}\text{C min}^{-1}$ until the temperature at the surface of the sample reached the desired. This slow ramping of the temperature prevents the temperature from over shooting. The hardness was then monitored until a plateau was reached in the hardness value, or a constant behaviour was observed for more than 30 min.

In the next few sections only reference to H_{\perp} will be made as it represents the plastic deformation mode within the fibrous structure of the material and is related to the inter-chain stacking necessary for the formation of the smectic mesophase and/or the triclinic crystals, whereas $H_{//}$ represents the deformation taking place in the direction of the draw.

Development of mesophase and crystallinity in PET

Figure 5a shows H_{\perp} , in MPa, versus time, in minutes, for different PET samples drawn to a draw ratio of 3.5. It is clear from the figure that all samples show the same behaviour with a steep increase in hardness followed by a plateau. The time needed to reach the plateau increases with increasing the molecular weight of PET. This time is 20 min for PET 0.45 IV, $28,000\text{ g mol}^{-1}$, 30 min for PET 0.65 IV, $50,000\text{ g mol}^{-1}$ and 40 min for PET 0.90 IV, $82,000\text{ g mol}^{-1}$. It can be concluded that after this period

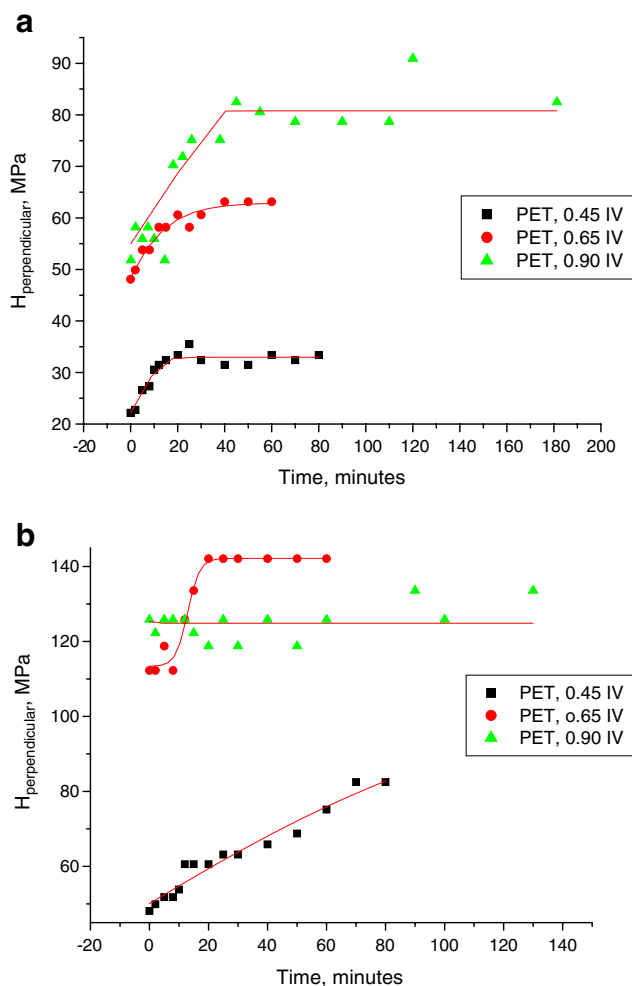


Fig. 5 The development of H_{\perp} as a function of time for different PET samples at 65 °C (a), smectic phase region, and 115 °C (b), triclinic region. [The red curves serve as a guide for the eye]

the amount of mesophase in the sample reaches maximum and this leads to the levelling off of the hardness values measured. It is relevant to note here that 65 °C is not high enough to induce crystallisation and this is confirmed by the X-ray measurements reported earlier [9].

Figure 5b shows the behaviour of the different PET samples at 115 °C, which is above T_g of PET so crystallisation can take place, and accordingly the kinetics of the crystallisation can be monitored. Interestingly, the behaviour of the three samples of PET is different. The lowest molecular weight PET sample shows a steady increase in hardness with time. The longer time needed by 0.45 IV PET to reach the plateau may be because it needs more time for densification to take place. On the other hand, the highest molecular weight PET seems to have reached the plateau of crystallinity already; the high molecular weight might have led to crystallisation to be completed at a lower temperature. The intermediate molecular weight PET requires 20 min to reach the

plateau, which means that the crystallinity increases gradually with a maximum value is attained after about 20 min at 115 °C.

Conclusions

Although PET is regarded as one of the most well known polymers; it is still regarded as a hot point of research inducing recent publications [22, 23]. From the results obtained in this paper it can be concluded that:

1. The microhardness of cold drawn PET samples exhibits an initial plateau at the beginning of annealing and then increase steeply as the material becomes reinforced, first by the presence of the smectic mesophase, and then the triclinic crystals. The mesophase in this case acts as a strong molecular network that reinforces the material and leads to increase in hardness values. This is opposed to the fact that in case of unoriented PET the hardness values decrease sharply at temperatures above T_g . Afterwards the hardness levels off when the maximum crystallinity is attained.
2. Indentation anisotropy (ΔH) is directly proportional to the amount of mesophase and oriented material present in the sample. It seems to be a valuable and effective measure of the degree of orientation of the sample. PET clearly exhibits maximum ΔH values at maximum degree of orientation.
3. The microhardness technique appears to be a valuable tool for studying the kinetics of the development of the mesophases, and the crystallinity of oriented polymer samples, this comes in agreement with recent publications relating both techniques [24].

References

1. Bonart R (1966) *Koll Z Z Polym* 210:16 213:1 (1966), and 231:438 (1967)
2. Imai M, Kaji K, Kanaya T, Sakai Y (1995) *Phys Rev B* 52 (17):12696
3. Auriemma F, Corradini P, DeRosa C, Guerra G, Petraccone V, Bianchi R, DiDino G (1992) *Macromolecules* 25:2490
4. Nicholson TM, Davis GR, Ward IM (1994) *Polymer* 35(20):4259
5. Welsh GE, Blundell DJ, Windle AH (1998) *Macromolecules* 31:7562
6. Welsh GE, Blundell DJ, Windle AH (2000) *J Mater Sci* 35:5225
7. Mahndasigam A, Martin C, Fuller W, Blundell DJ, Oldman RJ, Harvie JL, MacKerron DH, Riekel C, Engstrom P (1999) *Polymer* 40:5553
8. Blundell DJ, Mahendrasingam A, Martin C, Fuller W (2000) *J Mater Sci* 35:5057
9. Abou-Kandil AI, Windle AH (2007) *Polymer* 48(17):5069
10. Abou-Kandil AI, Windle AH (2007) *Polymer* 48(16):4824
11. Abou-Kandil AI, Windle AH (2007) *Macromolecules* 40(18):6448
12. Asano T, Balta Calleja FJ, Flores A, Tanigaki M, Mina MF, Sawatari C, Itagaki H, Takahashi H, Hatta I (1999) *Polymer* 40:6475
13. Balta-Calleja FJ (1985) *Adv Polym Sci* 66:117
14. Vanderdonckt C, Krumova M, Balta Calleja FJ, Zachmann HG, Fakirov S (1998) *Colloid Polym Sci* 276:138
15. Berkowitz S (1984) *J Appl Polym Sci* 29:4353
16. Verma RK, Hsiao BS (1996) *Trends Polym Sci* 4:312
17. Balta-Calleja FJ, Fakirov S (2000) *Microhardness of polymers*. Cambridge University Press, Cambridge
18. Balta Calleja FJ, Rueda DR, Porter RS, Mead WT (1980) *J Mater Sci* 15:765
19. Santa Cruz C, Balta Calleja FJ, Zachmann HG, Stribeck N, Asano T (1991) *J Polym Sci Part B Polym Phys* 29:819
20. Kajaks J, Flores A, Garcia Gutierrez MC, Rueda DR, Balta Calleja FJ (2000) *Polymer* 41:7769
21. Balta Callega FJ, Santa Cruz C, Asano T (1993) *J Polym Sci Part B Polym Phys* 31:557
22. Hsu G-H, Yang Y-N, Yu TL, Lin H-L (2006) *J Polym Res* 13:361
23. Ren M, Zhang Z, Wu S, Wei J, Xiao C (2006) *J Polym Res* 13:9
24. Uchiyama T, Suyama M, Alam MM, Asano T, Henning S, Flores A, Balta-Calleja FJ, Mina MF (2007) *Polymer* 48:542